Synthesis and Luminescence Properties of Monophasic Organic−Inorganic Hybrid Materials Incorporating Europium(III)

Frank Embert, Ahmad Mehdi, Catherine Reyé, and Robert J. P. Corriu*

Laboratoire de Chimie Moleculaire et Organisation du Solide, UMR 5637 CNRS, Université de Montpellier II, Sciences et Techniques du Languedoc, Place E. Bataillon, F-34095 Montpellier Cedex 5, France

Received March 8, 2001. Revised Manuscript Received July 12, 2001

Phosphine oxides **1**−**5** bearing one, two, or three hydrolyzable $Si(OR)_3$ groups have been prepared. They were treated with anhydrous europium salts [$Eu(NO_3)_3$ or $EuCl_3$] to afford complexes **6**−**10**, the stoichiometry of which was found to be one Eu^{3+} for three P═O centers. The hydrolytic polycondensation of these complexes gave rise to nanostructured hybrid materials incorporating Eu^{3+}. A solid-state ^{31}P NMR study of these hybrid materials has shown that Eu^{3+} remains well encapsulated within the materials when they are prepared from europium complexes with phosphine oxides bearing one hydrolyzable $Si(OR)_3$ group. The luminescence behavior of these materials has been investigated. At room temperature, a very strong red emission was observed. The study of the emission lines at 2 K strongly suggested that there was predominantly one Eu^{3+} binding site within the materials.

Introduction

The incorporation of luminescent centers into silica gels has been a challenge for a number of research groups. Indeed, materials with stable and highly luminescent properties could give rise to many applications including fiber amplifiers and solid-state lasers.[1,2] The sol−gel route is an attractive means of synthesizing such materials since it allows processing into thin films, fibers, or monoliths.[3,4] For these reasons, silicate glasses doped with rare-earth cations have been extensively investigated.[5−7] However, the luminescence efficiency of rare-earth ions in sol−gel host materials is currently limited by hydroxyl quenching[8−11] originating in residual water, silanol groups, and dopant clustering.[12−14] Among the various techniques for alleviating these drawbacks,[3,4,12,15−18] the embedding of rare-earth organic complexes in silica gels[19−25] by using the sol−gel process has been much investigated recently. The resulting organic−inorganic hybrid optical materials were shown to exhibit notably improved luminescence properties with respect to simple metal ions in silica. Indeed, such organic complexes first increase the concentration of lanthanide salts in the inorganic matrix. Furthermore, the organic ligands protect the central lanthanide ions from silanol groups present in the silica matrix, thus diminishing nonradiative decay pathways of the rare-earth ions. Finally, lanthanide ions encapsulated by absorbing ligands can give rise to intramolecular energy transfer from the coordinating ligands to the central lanthanide ions, which in turn undergo the corresponding radiative emitting process ("the antenna effect").[26] However, this method gives rise to nanocomposite hybrid materials[27] (class I) in which the

* To whom correspondence should be addressed. E-mail: corriu@crit.univ-montp2.fr.

(1) Weber, M. J. *J. Non-Cryst. Solids* **1990**, *123*, 208.
(2) Klein, L. C. *Annu. Rev. Mater. Sci.* **1993**, *23*, 437.
(3) Yuh, S.; Bescher, E. P.; Babonneau, F.; Mackensie, J. D. In *Better Ceramics Through Chemistry VI*; Cheetham, A. K., Brinker, C. J., Mecartney, M. L., Sanchez, C., Eds.; Materials Research Symposium Series; Materials Research Society: Pittsburgh, 1994; Vol. 346, p 803.
(4) Sanchez, C.; Lebeau, B.; Viana, B. In *Sol−Gel Optics III*; Mackensie, J. D., Ed.; SPIE Proceedings Series; SPIE: Bellingham, WA, 1994; Vol. 2288, p 227.
(5) Levy, D.; Reisfeld, R.; Avnir, D. *Chem. Phys. Lett.* **1994**, *109*, 593.
(6) Lecomte, M.; Viana, B.; Sanchez, C. *J. Chem. Phys.* **1991**, *88*, 39.
(7) Lochhead, M. J.; Bray, K. L. *J. Non-Cryst. Solids* **1994**, *170*, 143.
(8) Pope, E. J. A; Mackensie, J. D. *J. Non-Cryst. Solids* **1988**, *106*, 236.
(9) Thomas, I. M.; Payne, S. A.; Wilke, G. D. *J. Non-Cryst. Solids* **1992**, *151*, 267.
(10) Chakrabarti, S.; Sahu, J.; Chakraborti, M; Acharya, H. N. *J. Non-Cryst. Solids* **1994**, *180*, 96.
(11) Viana, B.; Koslova, N.; Ashehoug, P.; Sanchez, C. *J. Mater. Chem.* **1995**, *5*, 719.
(12) Lochhead, M. J.; Bray, K. L. *Chem. Mater.* **1995**, *7*, 572.
(13) Costa, V. C.; Lochhead, M. J.; Bray, K. L. *Chem. Mater.* **1996**, *8*, 783.
(14) Kurokawa, Y.; Ishizaka, T.; Ikoma, T.; Tero-Kwbota, S. *Chem. Phys. Lett.* **1998**, *287*, 737.
(15) Brinker, C. J.; Scherer, G. W. *Sol−Gel Science*; Academic Press: Boston, 1990.
(16) Fujiyama, T.; Hori, M.; Sasaki, M. *J. Non-Cryst. Solids* **1990**, *121*, 272.
(17) Arai, K.; Namikawa, H.; Ishii, Y.; Imai, M.; Hosono, H. *J. Non-Cryst. Solids* **1987**, *95*, 609.
(18) Pope, E. J. A.; Mackensie, J. D. *J. Am. Ceram. Soc.* **1993**, *76*, 1325.
(19) Mattews, L. R.; Knobbe, E. T. *Chem. Mater.* **1993**, *5*, 1697.
(20) Yan, B.; Zhang, H. J.; Ni, J. Z. *Mater. Sci. Eng.* **1998**, *B52*, 123.
(21) Serra, O. A.; Nassar, E. J.; Zapparolli, G.; Rosa, I. L. V. *J. Alloys Compd.* **1994**, *207/208*, 454.
(22) Zhang, Y.; Wang, M.; Xu, J. *J. Mater. Sci. Eng.* **1997**, *B47*, 23.
(23) Serra, O. A.; Nassar, E. J.; Rosa, I. L. V. *J. Lumin.* **1997**, *72−74*, 263.
(24) Jin, T.; Inoue, S.; Tsutsumi, S.; Machila, K.; Adachi, G. *J. Non-Cryst. Solids* **1998**, *223*, 123.
(25) Jin, T.; Tsutsumi, S.; Deguchi, Y.; Machila, K.; Adachi, G. *J. Alloys Compd.* **1997**, *252*, 59.

10.1021/cm0101982 CCC: $20.00
Published on Web 11/13/2001

dispersion of emitting species is inhomogeneous. In addition, leaching of the lanthanide complexes that are not anchored to the silica matrix occurs. Another approach that should result in a homogeneous dispersion of the lanthanide cations within the hybrid materials consists of the hydrolysis and polycondensation of rare-earth complexes with ligands bearing hydrolyzable $Si(OR)_3$ groups. This method affords monophase organic−inorganic nanostructured hybrid materials[27,28] (class II) in which the organic ligand is covalently linked to the silica framework. Up to now and to the best of our knowledge, very few papers concerning the preparation of materials incorporating lanthanide ions by this route have been reported.[29,30] Indeed, it requires the synthesis of silylated ligands able to completely encapsulate the ions.

In the course of studying nanostructured hybrid materials, we have described the preparation of phosphines and phosphine derivatives bearing two or three hydrolyzable $Si(OR)_3$ groups and their hydrolysis and polycondensation.[31] We have shown the importance of the number of hydrolyzable $Si(OR)_3$ groups for the accessibility of phosphorus centers incorporated within the corresponding materials.[32] With a view to preparing hybrid materials with luminescence properties, we used the well-known binding ability of phosphine oxides toward the lanthanide ions[33,34] to prepare europium complexes with phosphine oxides bearing one, two, or three hydrolyzable $Si(OR)_3$ groups as ligands. Indeed, among the lanthanide ions, europium is a particularly attractive luminescent center due to its long-lived and narrow-width emission band.[26,35]

In this paper, we present a simple synthetic approach to highly efficient luminescent europium(III)-containing hybrid materials. These materials are obtained by hydrolysis and polycondensation via a sol−gel protocol of isolated Eu complex monomers. We have examined the influence of the number of $Si(OR)_3$ groups of the Eu complexes on the degree of encapsulation of Eu^{3+} within the resulting solids, and we describe the preparation of nanostructured hybrid materials in which the local environment around the emitting species is unique.

Experimental Section

All manipulations were carried out with standard high-vacuum and dry-argon techniques. The ^1H and ^{13}C NMR solution spectra were recorded on a Bruker DPX 200 (at 200 MHz for ^1H and 50 MHz for ^{13}C), the ^{31}P NMR spectra on a Bruker WP 250 SY (at 100 MHz), and the ^{29}Si NMR spectra on a Bruker AC 200 (at 40 MHz). Chemical shifts (δ, ppm) were referenced to Me_4Si (^1H, ^{13}C, ^{29}Si) or H_3PO_4 (^{31}P). The abbreviations used are s for singlet, d for doublet, t for triplet, q for quartet, sept for septet, and m for multiplet.

Cross-polarization magic angle spinning (CP MAS) ^{29}Si NMR spectra were recorded on a Bruker FTAM 300 as were CP MAS ^{13}C NMR spectra. In both cases, the repetition times were 5 and 10 s with contact times of 5 and 2 ms. The HPDEC MAS ^{31}P NMR spectra were recorded on a Bruker FTAM 300, a Bruker ASX 200, or a Bruker ASX 400 with a repetition time of 5 s. IR spectra were recorded on a Perkin-Elmer 1600 spectrometer. Fast atom bombardment (FAB) mass measurements [matrix *m*-nitrobenzyl alcohol (NBA)] were registered on a JEOL JMS-D3000 spectrometer. Specific surface areas were determined by the Brunauer−Emmett−Teller (BET) method on Micromeritics ASAP 2010 and Micromeritics Gemini III 2375 analyzers. Melting points were measured with a Büchi B-540. Microanalyses were performed by the Service Central d'Analyse (CNRS, France). $Eu(NO_3)_3{\cdot}6H_2O$ and $EuCl_3{\cdot}6H_2O$ were purchased from Across. Compound **1**[31] was prepared according to the published procedure. Photoluminescence measurements were performed at low temperature (2 K) using the 325 nm radiation of a He−Cd laser as excitation source operating at a power of 10 mW. Sample cooling was provided by a closed-cycle He optical cryostat (Cryomech GB-15). Excitation spectra were recorded using a Xe lamp.

Preparation of Diphenyl[*p*-(triisopropoxysilyl)phenyl]phosphine. The Grignard reagent of the (*p*-bromophenyl)-triisopropoxysilane was prepared as described in the literature[31] from 2.01 g of magnesium (82.5 mmol) and 28.46 g of the bromide derivative in 120 mL of THF. A 100 mL sample of a THF solution of chlorodiphenylphosphine (16.57 g, 75.1 mmol) was added dropwise at 0 °C to the Grignard reagent. The reaction mixture was stirred at room temperature for one night and then heated under reflux for 1 h. After removal of the solvent, the pasty residue was dissolved in pentane. The mixture was filtrated, and the precipitate was washed with pentane. The filtrate was concentrated, and a colorless oil was obtained which was crystallized from 2-propanol. After filtration and washing with cool 2-propanol, 27.5 g of a white solid was isolated: yield 78%; mp 36.6−37.1 °C; ^1H NMR ($CDCl_3$, 200 MHz) δ (ppm) 7.70−7.65 (m, 2H, H_6), 7.38−7.27 (m, 12H, $H_{3,4,5,7}$), 4.31 (sept, $^3J_{HH} = 6.1$ Hz, 3H, H_9), 1.24 (d, $^3J_{HH} = 6.1$ Hz, 18H, H_{10}); ^{13}C NMR ($CDCl_3$, 50 MHz) δ (ppm) 139.7 (d, $^1J_{PC} = 11.4$ Hz, C_2), 137.5 (d, $^1J_{PC} = 10.9$ Hz, C_1), 135.3 (d, $^3J_{PC} = 6.4$ Hz, C_5), 134.4 (d, $^2J_{PC} = 19.6$ Hz, C_4), 133.8 (s, C_8), 132.8 (d, $^2J_{PC} = 12.5$ Hz, C_3), 129.0 (d, $^3J_{PC} = 7.0$ Hz, C_7), 66.0 (s, C_9), 26.0 (s, C_{10}); ^{31}P NMR ($CDCl_3$, 100 MHz) δ (ppm) −4.61 (s); ^{29}Si NMR ($CDCl_3$, 40 MHz) δ (ppm) −61.81 (s); MS (FAB^+) $m/z = 467$ ($M^+ + 1$, 100).

Preparation of Phosphine Oxides 2−5. The phosphine oxides **2**−**5** were prepared from the corresponding phosphines[31,36] according to a procedure that we have previously described,[31] and their physical data are reported in the Supporting Information.

Dehydration of Europium Salts. All the europium salts were dehydrated in the same way, by chemical reaction between the hydrated salt and ethyl orthoformate.[37] Dehydration of europium nitrate is given as an example. A 3 g (6.5 mmol) sample of $Eu(NO_3)_3{\cdot}6.7H_2O$ was dissolved in 40 mL of anhydrous ethanol. This solution was placed in a two-necked flask. A 7.04 g (47.6 mmol) sample of ethyl orthoformate was added at room temperature with a syringe to this ethanolic solution. The mixture was heated so that azeotrope ethyl formate/ethanol distilled drop by drop ($T = 78$ °C). The reaction was monitored by ^1H NMR spectroscopy. When the formation of ethyl formate was done, the residual ethanol was removed under vacuum to give 2.36 g of a beige solid. A Karl Fisher titration of a 0.05 M $Eu(NO_3)_3$ solution in anhydrous ethanol afforded $Eu(NO_3)_3{\cdot}0.09H_2O$.

Synthesis of Phosphine Oxide−Europium Salt Complexes 6−10. Complexes **6**−**10** were prepared in the same

(26) Sabbatini, N.; Guardigli, M.; Lehn, J.-M. *Coord. Chem. Rev.* **1993**, *123*, 201.
(27) Sanchez, C.; Ribot, F. *New J. Chem.* **1994**, *18*, 1007.
(28) Corriu, R. J. P. *Angew. Chem., Int. Ed.* **2000**, *39*, 1376.
(29) Franville, A.-C.; Zambon, D.; Mahiou, R.; Troin, Y. *Chem. Mater.* **2000**, *12*, 428.
(30) Dong, D.; Jiang, S.; Men, Y.; Ji X.; Jiang, B., J. *Adv. Mater.* **2000**, *12*, 646.
(31) Bezombes, J.-P.; Chuit, C.; Corriu, R. J. P.; Reyé, C. *J. Mater. Chem.* **1998**, *8*, 1749.
(32) (a) Bezombes, J.-P.; Chuit, C.; Corriu, R. J. P.; Reyé, C. *J. Mater. Chem.* **1999,** *9*, 1727. (b) Bezombes, J.-P.; Chuit, C.; Corriu, R. J. P.; Reyé, C. *Can. J. Chem.* **2000**, *78*, 1519.
(33) Cousins, D. R.; Hart, F. A. *J. Inorg. Nucl. Chem.* **1967**, *29*, 1745.
(34) Valle, G.; Casotto, G.; Zanonato, P. L.; Zarli, B. *Polyhedron* **1986**, *5*, 2093.
(35) Bunsli, J.-C. G.; Choppin, G. R. *Lanthanide Probes in Life, Chemical, and Earth Sciences*; Elsevier: New York, 1989.
(36) Behringer, K. D.; Blümel, J. *Inorg. Chem.* **1996**, *35*, 1814.
(37) Almasio, M.-C.; Arnaud-Neu, F.; Schwing-Weill, M.-J. *Helv. Chim. Acta* **1983**, *66*, 1296.

Table 1. ^{13}C, ^{31}P, and ^{29}Si NMR Chemical Shifts (δ, ppm) for Hybrid Materials Incorporating Eu^{3+} Salts

material	^{13}C CP MAS	^{31}P HPDEC MAS	^{29}Si CP MAS
$\mathbf{X_A8}$	131.3	30.8 (15%), −112.9 (85%)	−69.7
$\mathbf{X_A9a}$	132.0	33.0 (22%), −108.5 (78%)	−69.7
$\mathbf{X_A9b}$	131.3	30.3 (21%), −117.3 (79%)	−68.7
$\mathbf{X_A10a}$		35.2 (10%), −108.5 (90%)	−55.2
$\mathbf{X_F10a}$	128.6, 10−25	38.8 (15%), −108.0 (85%)	−57.8
$\mathbf{X_A10b}$		32.1 (9%), −87.6 (91%)	

way, according to a procedure described in the literature:[33] A boiling ethanolic solution of europium salt (50 mmol L^{-1}) was treated with 3 equiv of phosphine oxide in boiling ethanol (solution 0.2 M). There was at once formation of a white precipitate. Attempts to recrystallize europium complexes did not succeed. Therefore, in so far as no impurity was evident from the different analyses, the crude europium complexes were used. Their physical data are reported in the Supporting Information.

Synthesis of Phosphine Oxide−Gadolinium Nitrate Complex 11. 11 was prepared as the europium complex: mp 87.0−88.7 °C; IR (cm^{-1}, DRIFT) 1482.8 [ν(N−O)], 1306.6 [ν_{as}-(NO_2)], 1440.2 [δ(P−C_{sp2})], 1162.4 [ν(P=O···Gd^{3+})], 1119.7, 1082.3 [δ(Si−O)], 815.2 [δ_{hp}(NO_2)]; MS (FAB$^+$, NBA) m/z = 1602 [(M + H)$^+$ − NO_3, 55], 1162 [(M + H)$^+$ − NO_3 + P=O), 100], 722 [(M + H)$^+$ − (2NO_3 + 2P=O), 12], 441 [(P=O)$^+$, 20]. Anal. Calcd for $C_{72}H_{87}GdN_3O_{21}P_3Si_3$: C, 51.94; H, 5.27; Gd, 9.45; P, 5.58; N, 2.52; Si, 5.06. Found: C, 51.44; H, 5.06; Gd, 8.90; P, 5.25; N, 2.39; Si, 5.80.

Preparation of Xerogels. The hydrolysis and polycondensation of different europium(III) complexes and that of the gadolinium complex **11** have been carried out according to the same procedure. The xerogels are named $\mathbf{X_z N.}$ **X** indicates xerogel. The index z = **A** or **F** specifies the catalyst of gelification, **A** to denote 10% HCl as catalyst and **F** to denote 10 mol % TBAF as catalyst. ***N*** indicates the number that characterizes the phosphine oxide. ^{31}P, ^{13}C, and ^{29}Si NMR data of the xerogels are given in Table 1, and the other physical data are given below. The preparation of $\mathbf{X_A10a}$ is given as an example.

X_A10a. A solution of **10a** (1.50 g, 0.96 mmol) in THF (1.45 mL) was placed in a 35 mL Pyrex test tube. A 0.96 mL sample of a THF solution, 4.5 M in H_2O (4.34 mmol) and 0.1 M in HCl (10 mol %), was added dropwise at room temperature with a syringe. After 3 min of stirring, the solution was placed in a thermostated water bath at 30 °C without stirring. After 20 h, a gel was formed. The wet white opaque gel was allowed to age for 5 days at 30 °C, after which it was powdered and washed with acetonitrile and ether. The gel was powdered again and dried under vacuum (0.1 mmHg) for 13 h at 120 °C, yielding 1.05 g of a white powder: thermogravimetric analyses (TGA) [weight loss, % (T, °C)] 2.0 (150−230), 10.8 (230−340), 8.0 (340−660), 3.1 (1040−1250); IR (DRIFT, KBr, cm^{-1}) 3466 [ν(O−H)], 1472 [ν(N−O)], 1301 [ν_{as}(NO_2)], 815 [γ_{hp}(NO_2)], 740 [γ(NO_2)].

Data for **X_A6.** IR (DRIFT, KBr, cm^{-1}) 3338 [ν(O−H)], 1504, 1467 [ν(N−O)], 1291 [ν_{as}(NO_2)], 815 [γ_{hp}(NO_2)]. Anal. Calcd for $C_{54}EuH_{36}N_3O_{22.5}P_3Si_9$ (Found): C, 40.93; Eu, 9.59; H, 2.29; N, 2.65; P, 5.86; Si, 15.95 (i.e., $C_{79.4}Eu_{0.8}H_{116}N_{2.2}P_{2.9}Si_{9.0}$).

Data for **X_A7.** IR (DRIFT, KBr, cm^{-1}) 3615, 3241 [ν(O−H)], 1472 [ν(N−O)], 1312 [ν_{as}(NO_2)], 815 [γ_{hp}(NO_2)]. Anal. Calcd for $C_{54}EuH_{39}N_3O_{21}P_3Si_6$ (Found): C, 43.84; Eu, 10.28; H, 2.66; N, 2.84; P, 6.28; Si, 11.39 (i.e., $C_{53.7}Eu_{1.1}H_{59.2}N_{2.8}P_{3.0}Si_{5.8}$).

Data for **X_A8.** TGA [weight loss, % (T, °C)] 25.1 (150−600), 6.9 (600−800), 2.3.0 (1100−1150); IR (DRIFT, KBr, cm^{-1}) 3626 [ν(O−H)], 1483 [ν(N−O)], 1301 [ν_{as}(NO_2)], 815 [γ_{hp}(NO_2)], 740 [γ(NO_2)].

Data for **X_A9a.** IR (DRIFT, KBr, cm^{-1}) 3615 [ν(O−H)], 1488 [ν(N−O)], 1296 [ν_{as}(NO_2)], 815 [γ_{hp}(NO_2)], 740 [γ(NO_2)].

Data for **X_A9b.** ^{31}P (162 MHz, HPDEC MAS) δ (ppm) 30.8 (P=O, 16), −82.8 (P=O···Eu^{3+}, 84).

Data for **X_F10a.** IR (DRIFT, KBr, cm^{-1}) 3498 [ν(O−H)], 1478 [ν(N−O)], 1307 [ν_{as}(NO_2)], 815 [γ_{hp}(NO_2)], 740 [γ(NO_2)].

Chart 1

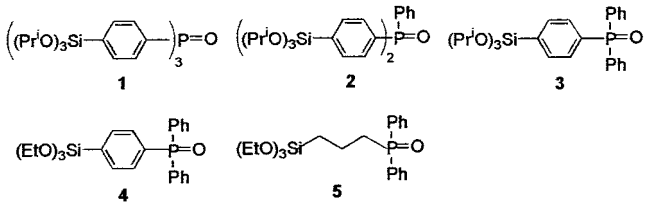

Chart 2

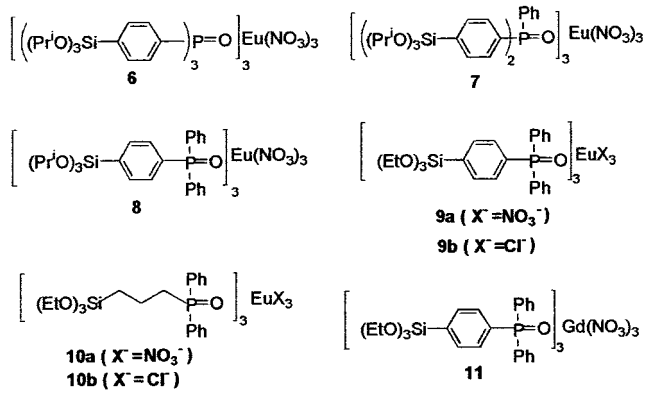

Data for **X_A10b.** TGA [weight loss, % (T, °C)] 2.3 (150−450), 35.7 (450−500), 12.9.0 (500−700), 34.8.0 (700−1000); IR (DRIFT, KBr, cm^{-1}) 3626, 3327 [ν(O−H)].

Data for **X_A11.** TGA [weight loss, % (T, °C)] 1.8 (150−200), 6.0 (200−350), 50.3 (350−650), 2.9 (650−1000); IR (DRIFT, KBr, cm^{-1}) 3637, 3316 [ν(O−H)], 1483 [ν(N−O)], 1301 [ν_{as}(NO_2)], 815 [γ_{hp}(NO_2)], 740 [γ(NO_2)]. Anal. Calcd for $C_{54}H_{42}$-$GdN_3O_{16.5}P_3Si_3$ (Found): C, 48.72; H, 3.58; Gd, 11.00; N, 2.66; P, 7.25; Si, 5.80 (i.e., $C_{51.4}H_{40.4}Gd_{0.9}N_{3.1}P_{3.0}Si_{2.8}$).

Results and Discussion

Preparation and Characterization of Eu−Phosphine Oxide Complexes. We have prepared as organic ligands the phosphine oxides **1**,[31] **2,** and **3** bearing, respectively, three, two, and one hydrolyzable $Si(OPr^i)_3$ groups (Chart 1). As our purpose was to obtain very well condensed materials to eliminate nonradiative deactivation owing to the remaining SiOH groups, we have also prepared the ligand **4** and the more flexible phosphine oxide **5**, both of them bearing one $Si(OEt)_3$ group. Attempts to isolate Eu complexes by reaction of silylated phosphine oxides with hydrated europium salts (nitrate or chloride) failed. Indeed, during the complexation, a partial hydrolysis of $Si(OPr^i)_3$ groups took place. The hydrolysis was substantial for the ligands **4** and **5** bearing one $Si(OEt)_3$ group. That was probably due to the Lewis acid character of rare-earth ions that catalyzes the hydrolysis. Thus, to isolate pure Eu complexes, complete dehydration of the europium salts was required. This was achieved by reaction of the hydrated salts with ethyl orthoformate,[37] thermal dehydration of europium salts being incomplete even after 48 h at 150 °C under 0.1 Torr.

Treatment of an alcoholic solution (2-propanol or ethanol depending on the nature of the hydrolyzable group) of anhydrous europium salts EuX_3 (nitrate or chloride) with 3 equiv of the silylated phosphine oxides **1**−**5** afforded the corresponding tris(phosphine oxide)−europium salt complexes **6**−**10** (Chart 2) in high yield.[33] All of them have been fully characterized by spectro-

Table 2. ^{31}P NMR Chemical Shifts (δ, ppm) for Phosphine Oxides, Europium−Phosphine Oxide Complexes, and the Corresponding Xerogels

phosphine oxide[a]		$Eu(NO_3)_3$ complex[a]		xerogel[b]	
1	29.8	**6**	**−111.7**	$\mathbf{X_A6}$	26.7 (68%), −133.4 (32%)
2	30.4	**7**	**−115.3**	$\mathbf{X_A7}$	32.6 (76%), −125.0 (24%)
3	29.6	**8**	**−114.8**	$\mathbf{X_A8}$	30.8 (13%), −112.9 (87%)
4	29.3	**9a**	**−115.1**	**X9a**	33.0 (22%), −108.5 (78%)
5	32.3	**10a**	**−107.3**	**X10a**	35.2 (10%), −108.5 (90%)

[a] In $CDCl_3$. [b] ^{31}P NMR (HPDEC).

scopic methods as detailed in the Experimental Section. Integration of the ^{1}H NMR signals reveals that no hydrolysis of isopropoxy or ethoxy groups occurred during the complexation reaction. The ^{31}P NMR spectrum of each complex displays only one broad signal that is notably shifted upfield in comparison to that of the starting ligand ($|\Delta\delta| \approx 140$ ppm), indicating that all the phosphine oxide has reacted (Table 2). Further evidence for complete reaction was given by FTIR experiments. Indeed, no free P═O stretching vibration was observed. The P═O stretching vibration in the complexes is shifted to a lower frequency (30−50 cm^{-1}; see the Experimental Section) than that of the corresponding free ligand, indicating that the coordination of these subunits to the europium ions occurred in the complexes. These values are in good agreement with the literature data.[33] The FTIR spectra of the europium nitrate complexes **6**−**8**, **9a**, and **10a** exhibit N−O and asymmetric NO_2 stretching bands which are very close to those obtained for the trinitrato−tris(triphenylphosphine oxide)−Eu^{3+} complexes.[33] As the X-ray structure of this complex has revealed that the europium(III) was coordinated to three bidentate nitrato groups in addition to three phosphine oxides,[34] we can conclude that the nitrato groups are also bidentate in our complexes. Finally, all the complexes that we have prepared were unambiguously characterized by FAB^+ mass spectroscopy.

Research on the Best Precursors for Hybrid Materials. First of all, the sol−gel process was performed on isolated silylated complexes **6**−**8** bearing, respectively, nine, six, and three hydrolyzable $Si(OPr^i)_3$ groups to determine the best candidate to afford hybrid materials in which the Eu^{3+} ions remain well encapsulated during the sol−gel process. All of them were hydrolyzed under the same experimental conditions (THF as solvent, 30 °C, 10 mol % HCl as catalyst). After the workup described in the Experimental Section, the xerogels $\mathbf{X_A6}$, $\mathbf{X_A7}$, and $\mathbf{X_A8}$ were obtained (the index **A** denotes 10 mol % HCl as catalyst). The BET surface areas were found to be very low (<10 $m^2\ g^{-1}$) in all cases. The solid-state ^{31}P NMR spectra of these xerogels displayed two resonances (Table 2); one was attributed to the P═O group of the free ligand, and the other signal, which appears upfield, was assigned to the complexed P═O groups. Integration of the signals (Table 2) revealed that a significant decomplexation of the europium salt occurred during the sol−gel process of the precursors **6** and **7** while 87% of the P═O centers remained complexed when **8** was used as the precursor. The loss of europium salt after washing for the xerogels $\mathbf{X_A6}$ and $\mathbf{X_A7}$ was confirmed by elemental analysis. Thus, decomplexation of europium salts occurs in proportion to the number of hydrolyzable $Si(OPr^i)_3$ groups of the precursor (respectively, nine and six for **6** and **7**). We consider that, for both of the precursors, this number is so high that, during the formation of the inorganic network, the polycondensation induces geometric constraints that lead to decomplexation of europium. This provides a further indication of the importance of the number of hydrolyzable groups of the precursor on the properties of the resulting materials.[32,38] As the complexation of europium(III) ions survives the sol−gel process when the phosphine oxide contains only one hydrolyzable group, we have exclusively studied the materials prepared by using this type of ligand (**3**−**5**).

Characterization of the Hybrid Materials Incorporating Eu^{3+} Ions Obtained by Hydrolitic Polycondensation of 8, 9a,b, and 10a,b. The experimental conditions of hydrolysis and polycondensation of isolated $EuCl_3$ or $Eu(NO_3)_3$ complexes prepared from phosphine oxides **3**, **4**, or **5** are detailed in the Experimental Section. Sol−gel polycondensation of these complexes was performed under acidic conditions with 10 mol % HCl or under nucleophilic conditions with 10 mol % tetrabutylammonium fluoride (TBAF). It is worth noting that the gelification times are notably shorter under acidic conditions than under nucleophilic conditions. As an example, the gelification of **9b** takes 2 h in the presence of 10 mol % HCl while 36 h is necessary for the gelification of the same complex in the presence of 10 mol % TBAF. That is probably due to the strong tendency of Eu^{3+} complexes to coordinate small anions such as F^-.[39,40] As a consequence, the quantity of F^- able to catalyze the hydrolysis should be reduced.

Whatever the catalyst, the nature of the hydrolyzable $Si(OR)_3$ groups (R = Et or Pr^i), or the nature of the ligand (flexible or not), the hybrid materials incorporating Eu^{3+} present the same features.

(1) All the solid-state ^{31}P NMR spectra of the xerogels display two resonances, as was observed for $\mathbf{X_A6}$, $\mathbf{X_A7}$, and $\mathbf{X_A8}$. The integration of signals allows the calculation of the percentage of complexed P═O groups. The results are given in Table 1. From the arithmetic average of the percentage of complexed P═O groups, it was found that 81% of the P═O groups remain complexed within the materials prepared by using ligands **3** and **4** and 91% by using the more flexible ligand **5**. This result shows that the more flexible the organic moiety within the material, the lower the decomplexation of the Eu^{3+} ions. This is in agreement with the results observed on the materials prepared from complexes **6**−**8**.

(2) The solid-state ^{29}Si NMR spectra of the xerogels (Table 1) display only one broad signal, centered at −70 ppm for the materials prepared by using ligands **3** and **4** and centered at −57 ppm for those prepared from **5**. Because of the poor resolution of the ^{29}Si NMR spectra due to the presence of the europium salts, it was not possible to give an estimation of the degree of condensation of the material. Furthermore, as no signal appears between −90 and −110 ppm in all cases, it can be

(38) Dubois, G.; Reyé, C.; Corriu, R. J. P.; Chuit, C. *J. Mater. Chem.* **2000**, *10*, 1091.
(39) Ganson, O. A.; Kausar, A. R.; Weaver, M. J.; Lee, E. L. *J. Am. Chem. Soc.* **1977**, *99*, 7087.
(40) Lee, E.; Ganson, O. A.; Weaver, M. J. *J. Am. Chem. Soc.* **1980**, *102*, 2278.

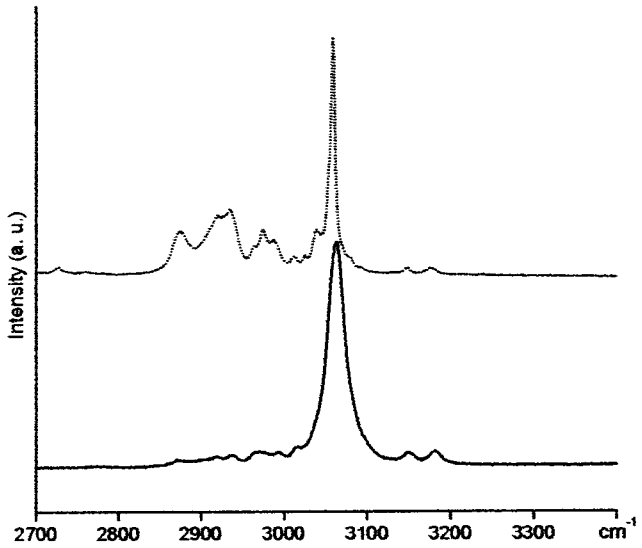

Figure 1. Solid-state Raman spectra in the 2700−3400 cm^{-1} range of **X1** (---) and of $\mathbf{X_A}$**9a** (—).

concluded that there is no cleavage of Si−C bonds during the sol−gel process.

(3) Solid-state ^{13}C NMR spectroscopy shows (Table 1) that there is no remaining ethoxy or isopropoxy groups whatever the nature or the quantity of the catalyst, indicating thus that the hydrolysis was complete. The signals at around 130 ppm were attributed to carbon of aromatic rings and the upfield signals (δ 10−25 ppm) to aliphatic carbons of ligands **10**. Confirmation of the complete hydrolysis of the precursors was given by Raman spectroscopy. The solid-state Raman spectrum of $\mathbf{X_A}$**9a** is given as an example. It reveals the absence of CH stretching bands between 2850 and 2970 cm^{-1} as indicated in Figure 1. For comparison, we have also reported in Figure 1 the Raman spectrum of the material **X1** prepared by hydrolysis and polycondensation of **1,** the degree of condensation of which had been found to be 59%.[31]

(4) The complete elemental analysis for some of the materials has been done. These data (Table 3) reveal that the degree of condensation of the materials is very high, which is very important for their luminescence properties. Furthermore, these data show that there is no loss of europium salts by washing of the materials with different solvents, which is a further indication of the encapsulation of the Eu^{3+} ions by the P═O groups within the materials.

(5) All the materials incorporating $Eu(NO_3)_3$ show in their solid-state Raman and IR spectra the same bands attributed to nitrate ions. As shown in Figure 2, the Raman spectrum of $Eu(NO_3)_3{\cdot}6H_2O$ displays in the 1020−1070 cm^{-1} range two absorptions bands located at 1047.4 and 1037.5 cm^{-1}. The band at 1047.4 cm^{-1} was assigned to the symmetric stretching band of water-solvated nitrate ions, and the other at 1037.5 cm^{-1} was attributed to a vibration of a contact $Eu^{3+}NO_3^-$ ion pair.[41] In contrast, the Raman spectrum of $\mathbf{X_A}$**8**, which was given as an example in Figure 2, exhibits in the same region of the spectrum only the band at 1037.5 cm^{-1}. Thus, it appears that the contact ion pair $Eu^{3+}NO_3^-$ survives the sol−gel process. The absence of the stretching vibration at 1047.4 cm^{-1} denotes the absence of hydrogen bonding between NO_3^- and either water molecules or OH vibrators. This was corroborated by FTIR measurements. Indeed, the most noteworthy features in the infrared spectra are the absorption band at 741 cm^{-1}, which is diagnostic of contact between nitrate and Eu^{3+} ions,[42] and the vibration at 815 cm^{-1}, which also denotes the absence of hydrogen bonding around nitrate ions.[43] It is worth noting that this last vibration, which is very sensitive to perturbations due to hydrogen bonding with nitrato groups, appears at the same value (815 cm^{-1}) in the anhydrous starting complexes **6**−**8, 9a,** and **10a**. This is a further indication of the absence of water molecules around NO_3^- ions in the materials.

(6) N_2 BET surface areas were found to be very low (<10 $m^2\ g^{-1}$) in all cases.

(7) All of the materials are amorphous.

Preparation of Cogels. Evidence for Clustering. The preparation of hybrid materials incorporating Eu^{3+} was also investigated by cohydrolysis and polycondensation of 20 equiv of tetraethyl orthosilicate (TEOS) and of 1 equiv of **9a**. The cogelification was achieved at 30 °C in THF solution with a stoichiometric amount of H_2O and in the presence of 10 mol % HCl as the catalyst. The solid was washed with acetonitrile and ether, powdered, and dried. The solid-state ^{31}P NMR spectrum of the resulting cogel displayed only one signal at 31 ppm, which was attributed to the free ligand **4**. Thus, the cogelification of **9a** with 20 equiv of TEOS induces the complete decomplexation of Eu^{3+}, in contrast to the gelification of the same complex. Scanning electron micrographs of $\mathbf{X_A}$**9a** and of the corresponding cogel are given in Figure 3. The material $\mathbf{X_A}$**9a** appears homogeneous while the cogel clearly shows the formation of Eu^{3+} clustering that appears as bright points. Analysis of the bright points by fluorescence X-ray spectroscopy revealed a high percentage of europium (>80%) in comparison to the other parts of the material. Furthermore, the cogel presents no luminescence properties in contrast to the material $\mathbf{X_A}$**9a** (vide infra), which confirms the formation of Eu^{3+} clustering in that case. Thus, it appears that the cogelification of europium(III) complexes with TEOS is not a convenient route to prepare hybrid organic−inorganic materials exhibiting luminescence properties.

Luminescence Properties of Materials $\mathbf{X_A}$*N* (*N* = 8−10). The excitation spectra of all of the materials incorporating Eu^{3+} ions were obtained by monitoring the emission of the Eu^{3+} ions at 618 nm. All of the excitation spectra present two broad absorption bands in the 250−350 nm range assigned to $\pi-\pi^*$ transition in the aromatic groups. They are at 343 and 297 nm (Figure 4) for the materials prepared by using ligands **3** and **4**. For the materials prepared by using ligand **5**, the absorption bands are much less intense and appear at 338 and 279 nm. The excitation spectra also present sharp bands which are characteristic of Eu^{3+} ions. The main bands appear at 395, 466, and 536 nm. They were attributed, respectively, to $^7F_0 \rightarrow {}^5L_6$, $^7F_0 \rightarrow {}^5D_2$, and $^7F_0 \rightarrow {}^5D_1$ transitions. These transitions are always weak compared to the $\pi-\pi^*$ transition in the organic

(41) Irish, D. E.; Puzic, O. *J. Solution Chem.* **1981**, *10*, 377.

(42) Irish, D. E.; Davis, A. R. *Can. J. Chem.* **1968**, *46*, 943.

(43) Nelson, D. L.; Irish, D. E. *J. Chem. Phys.* **1971**, *54*, 4479.

Table 3. Elemental Analyses of Some Xerogels and Percentage of P=O···Eu^{3+} Centers within the Xerogels

xerogel	calcd stoichiometry	exptl stoichiometry	%P=O···Eu^{3+}
$\mathbf{X_A8}$	$C_{54}EuH_{42}N_3O_{16.5}P_3Si_3$	$C_{54.7}Eu_{1.0}H_{44.6}N_{2.9}O_{17.5}P_{3.0}Si_{3.0}$	85
$\mathbf{X_A9a}$	$C_{54}EuH_{42}N_3O_{16.5}P_3Si_3$	$C_{56.5}Eu_{1.0}H_{49.1}N_{2.8}O_{17.6}P_{3.6}Si_{3.0}$	78
$\mathbf{X_F9a}$	$C_{54}EuH_{42}N_3O_{16.5}P_3Si_3$	$C_{54.7}Eu_{1.0}H_{44.6}N_{2.9}O_{17.6}P_{3.0}Si_{3.0}$	79
$\mathbf{X_A10a}$	$C_{45}EuH_{48}N_3O_{16.5}P_3Si_3$	$C_{44.2}Eu_{1.0}H_{50.1}N_{2.6}O_{16.3}P_{3.0}Si_{2.8}$	90
$\mathbf{X_F10a}$	$C_{45}EuH_{48}N_3O_{16.5}P_3Si_3$	$C_{45.5}Eu_{1.0}H_{53.0}N_{2.9}O_{16.9}P_{3.5}Si_{3.0}$	85
$\mathbf{X_A10b}$			91

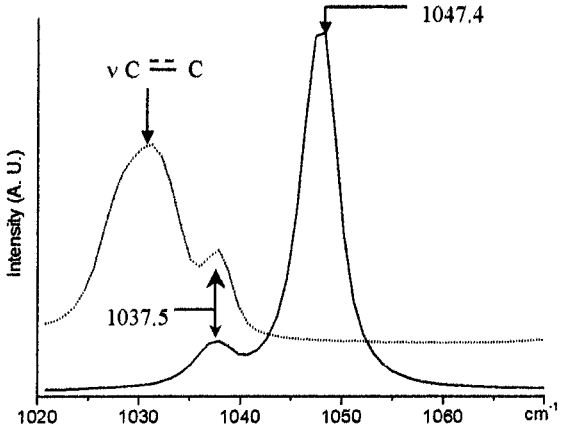

Figure 2. Solid-state Raman spectra of $Eu(NO_3)_3{\cdot}6H_2O$ (—) and of $\mathbf{X_A8}$ (---) in the 1020−1070 cm^{-1} range.

ligands. Thus, the luminescence via the excitation of the ligands is much more efficient than the direct excitation of the Eu^{3+} absorption levels.

The emission spectra of all the xerogels incorporating Eu^{3+} were recorded at room temperature either under a maximum of absorption of the ligand or by using the $^7F_0 \rightarrow {}^5L_6$ transitions of Eu^{3+} (395 nm). All the xerogels present the same type of emission spectra whatever the excitation wavelength, the nature of the ligand, or the salt [$Eu(NO_3)_3$, $EuCl_3$] (Figure 5). Eu^{3+} ions have five emission lines corresponding to the $^5D_0 \rightarrow {}^7F_i$ transitions, where $i = 0-4$. The strongest transition, $^5D_0 \rightarrow {}^7F_2$, occurs at 618 nm and is the characteristic "europium red" luminescence.

Antenna Effect. The emission spectra of different xerogels incorporating Eu^{3+}, being the same when using as the excitation wavelength either a maximum of absorption of the ligand or the $^7F_0 \rightarrow {}^5L_6$ transition of Eu^{3+} (395 nm), shows that the so-called "antenna effect" is operative.[26] In this indirect excitation mode, the factors that contribute to the luminescence intensity are

(i) the intensity of the ligand absorption,

(ii) the efficiency of the ligand-to-metal energy transfer, and (iii)

the efficiency of the metal luminescence. The absorption spectra of ligands **3**−**5** have been recorded in acetonitrile solution. In Table 4, the λ_{max} and the molar extinction coefficients ϵ are reported. As expected, ϵ values for **3** and **4** are superior to that of **5.** The same remark holds for the corresponding complexes (Table 4). The efficiency of the intramolecular energy transfer is very sensitive to the energy levels of the triplet state of the ligand. The closer the triplet-state levels of the ligand to the resonance energy level of the Eu^{3+} ion, the more efficient the intramolecular energy transfer. The gadolinium complex **11** (Chart 2) was prepared to determine the triplet-state energy levels (T) for ligand **4** as gadolinium complexes are known for their phosphorescence properties.[44] The excitation and emission

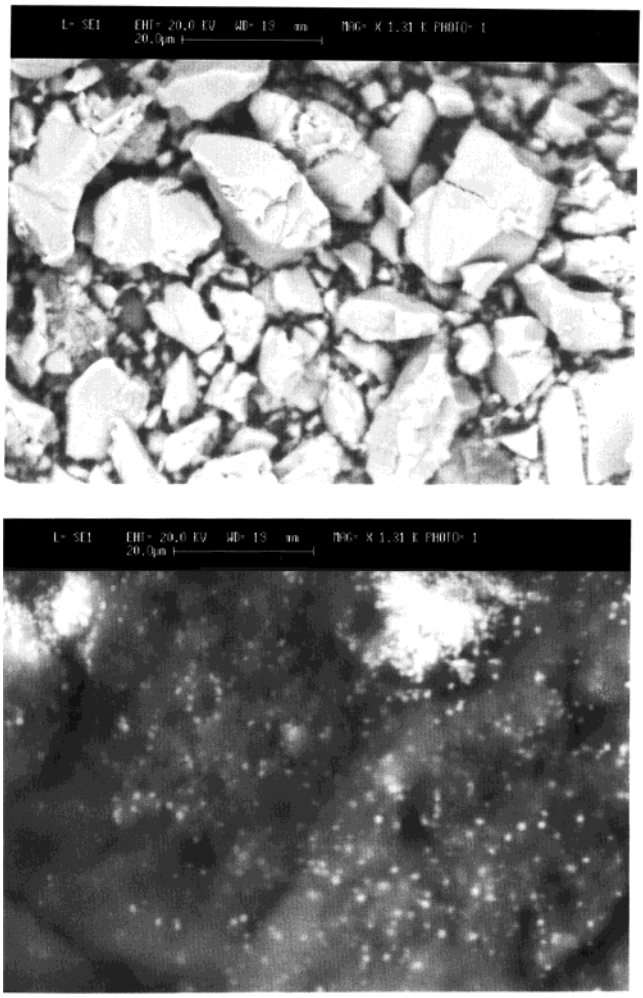

Figure 3. Scanning electron micrographs (top) for $\mathbf{X_A9a}$ and (bottom) for the material prepared by cogelification of **9a** with 20 equiv of TEOS.

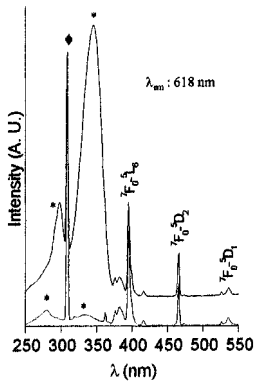

Figure 4. Excitation spectra at room temperature of $\mathbf{X_A9}$ (—) and of $\mathbf{X_A10a}$ (---): ♦, harmonic of the lamp; *, $^1\pi-\pi^*$.

spectra of the xerogel $\mathbf{X_A11}$ obtained by hydrolytic polycondensation of **11** are shown in Figure 6. It appears that the emission spectrum exhibited two broad phos-

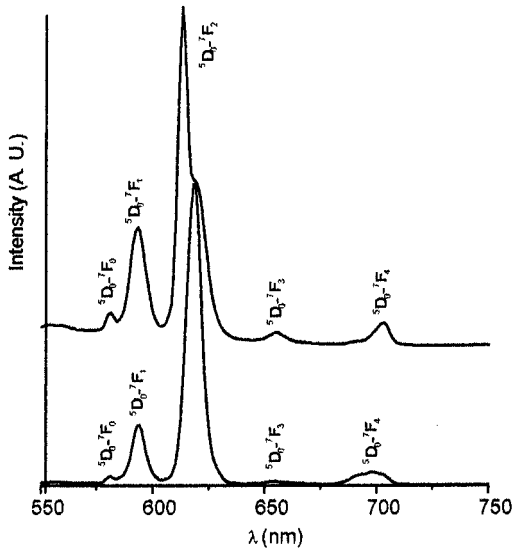

Figure 5. Emission spectra of xerogels $\mathbf{X}_A$**9a** (top) and $\mathbf{X}_A$**9b** (bottom) recorded under laser excitation at 343 and 395 nm at room temperature.

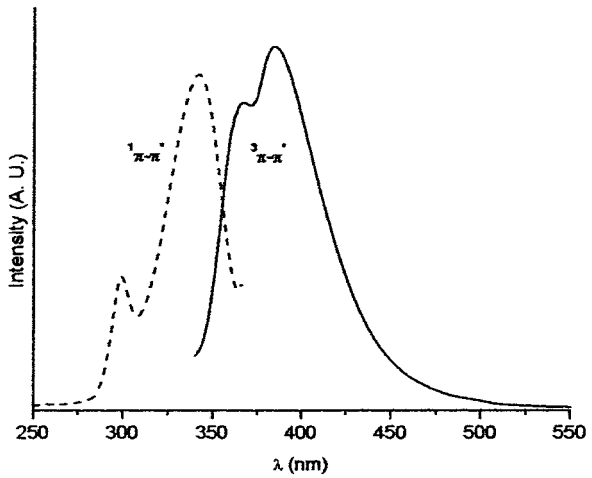

Figure 6. Excitation spectrum (---) at λ_{em} = 385 nm and emission spectrum (—) at λ_{exc} = 342 nm of $\mathbf{X}_A$**11**.

Table 4. Absorption Maxima and Molar Extinction Coefficients for Ligands 3−5 and Their Eu^{3+} Complexes 8−10

ligand or Eu^{3+} complex	λ_{max} (nm)	ϵ ($dm^3 \cdot mol^{-1} \cdot cm^{-1}$)	ligand or Eu^{3+} complex	λ_{max} (nm)	ϵ ($dm^3 \cdot mol^{-1} \cdot cm^{-1}$)
3	265.3	2070	**9b**	266.4	7040
8	266.2	6880	**5**	264.4	1040
4	265.3	2030	**10a**	265.3	4250
9a	266.3	6930	**10b**	265.3	4400

phorescence bands at 367 and 385 nm that correspond to the emission from the triplet states of the ligand. As Eu^{3+} presents excited states at 395 nm ($^7F_0$–$^5L_6$), 408 nm ($^7F_0$–$^5D_3$), and 380 nm ($^7F_0$–$^5G_2$), there is a perfect overlap between the excited state of the metal and the triplet-state level of ligand **4**. Furthermore, as the antenna effect corresponds to an intramolecular energy transfer which depends on the distance between the antenna (aromatic rings) and the metal center, we can expect intense luminescence for the materials prepared from **3** and **4** since the aromatic rings are located about

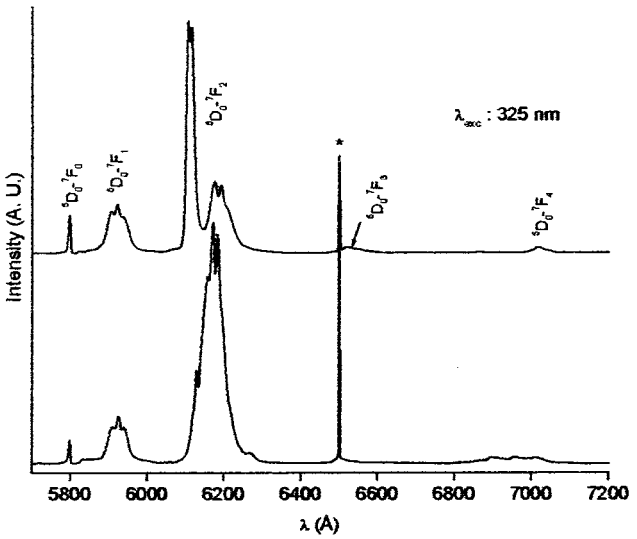

Figure 7. Emission spectra of xerogels $\mathbf{X}_A$**9b** (top) and $\mathbf{X}_A$**9a** (bottom) recorded under laser excitation at 325 nm at 2 K. The asterisk corresponds to second-order-scattered laser beams.

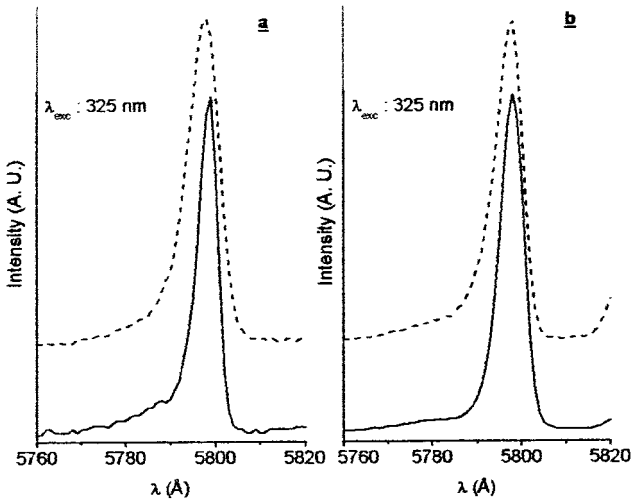

Figure 8. $^5D_0 \rightarrow {}^7F_0$ fluorescence spectra at 2 K under laser excitation at 325 nm of (a) $\mathbf{X}_A$**10a** (---) and $\mathbf{X}_A$**9a** (—) and (b) $\mathbf{X}_A$**10b** (---) and $\mathbf{X}_A$**9b** (—).

6 Å from the metal centers. Solid-state measurements of quantum yields have not been possible.

Photoluminescence at 2 K. It is known that the Eu^{3+} luminescence spectra exhibit an extraordinary sensitivity to the ligand environment.[45] Therefore, it was of interest to take advantage of the luminescent properties of our amorphous materials to have more information concerning the environment around the metal centers.

The luminescence of the xerogels was measured at 2 K under laser excitation at 325 nm. The emission spectra of all the xerogels exhibit the same features whatever the catalyst of gelification and the nature of the ligand (**3**, **4**, or **5**). In contrast, some differences appear according to the nature of the counteranions (NO_3^- or Cl^-). The spectra of $\mathbf{X}_A$**9a** and $\mathbf{X}_A$**9b** are given as examples in Figure 7. The line emission of xerogels incorporating Eu^{3+} ions were assigned to the transitions from the $^5D_0$ level to the ^7F_i levels (i = 0−4). The $^5D_0 \rightarrow$

(44) Latva, M.; Takalo, H.; Mukkala, V.-M.; Matachescu, C.; Rodriguez-Ubis, J. C.; Kankare, J. *J. Lumin.* **1997**, *75*, 149.

(45) Richardson, F. *Chem. Rev.* **1982**, *82*, 541.

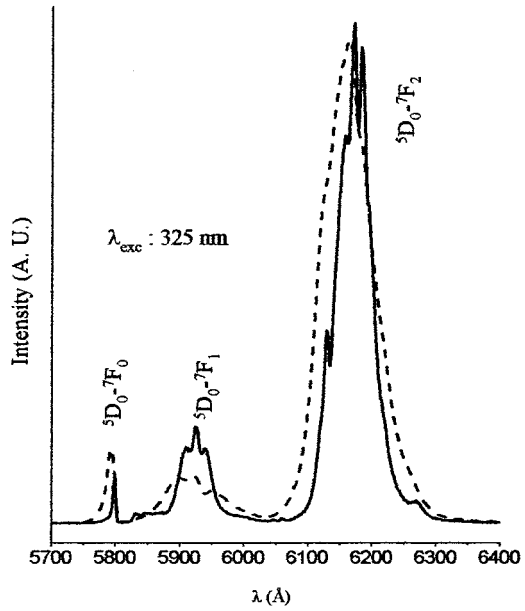

Figure 9. Emission spectra of xerogels $\mathbf{X_A9a}$ (—) and $\mathbf{X_A6}$ (---).

$^7F_2$ emission at 618 nm is the most important transition, which is in agreement with the amorphous character of the materials.[29] The most important probe transitions for Eu^{3+} complexes are $^5D_0 \rightarrow {}^7F_{0,1,2}$.[45] Indeed, the intensities of the $^5D_0 \rightarrow {}^7F_{0,1,2}$ lines are governed by selection rules which depend on the local symmetry of the crystal field around the ion. For systems in which there is only one type of Eu^{3+} binding site, the $^5D_0 \rightarrow {}^7F_1$ emission band can split at most into just three components and the $^5D_0 \rightarrow {}^7F_2$ emission band can split at most into just five components. As we did not observe, respectively, more than three and five splittings, it can be concluded that there is in our hybrid materials only one type of Eu^{3+} binding site. This was corroborated by the pattern of the $^5D_0 \rightarrow {}^7F_0$ emission, which can provide a better diagnostic probe for Eu^{3+} coordination homogeneity when observed with sufficient resolution.[45] Indeed, the $^7F_0$ energy level cannot be split by the crystal field; therefore, observation of more than one $^5D_0 \rightarrow {}^7F_0$ emission line at 2 K indicates the presence of more than one type of Eu^{3+}. This band for materials $\mathbf{X_AN}$ ($\boldsymbol{N}$ = **9a,b** or **10a,b**) is reported in Figure 8. In all cases, only one line is observed. This observation is in agreement with one type of Eu^{3+} binding site in our amorphous materials. Finally, we present in Figure 9 the emission spectrum of $\mathbf{X_A9a}$ in which 78% of P=O groups are coordinated to Eu^{3+} and that of $\mathbf{X_A6}$ in which only 24% of the P=O groups are coordinated, due to a partial decoordination induced by the polycondensation (vide supra). It is interesting to note that this difference between both materials involves a notable broadening of the $^5D_0 \rightarrow {}^7F_0$ and $^5D_0 \rightarrow {}^7F_1$ lines for the less homogeneous solid $\mathbf{X_A6}$. This is a further indication of the hypersensitive character of the $^5D_0 \rightarrow {}^7F_0$ and $^5D_0 \rightarrow {}^7F_1$ transitions to the ligand environment.

Conclusion

In this paper, we have shown that the hydrolysis and polycondensation of isolated Eu^{3+} complexes of phosphine oxides bearing one hydrolyzable $Si(OR)_3$ group afforded nanostructured hybrid materials in which Eu^{3+} ions are well encapsulated. This synthetic approach allowed the luminescence properties of Eu^{3+} within materials to be improved. Indeed, as the complexation survives the sol−gel process, clustering of the emitting species was thus prevented. It was shown that there were no OH groups coordinated to Eu^{3+} ions, which are strong deactivators reducing the luminescence intensity. The very interesting ability of the phosphine oxides with aromatic substituents to act as antennae in energy transfer was outlined. Finally, the study of luminescence properties of materials at 2 K has shown that there is predominantly one type of Eu^{3+} binding site within the materials.

Supporting Information Available: Physical data for compounds **2**−**10** (PDF). This material is available free of charge via the Internet at http://pubs.acs.org.

CM0101982